

Shape Control of Al Nanoclusters by Ligand Size

Hongjun Xiang,* Joongoo Kang, Su-Huai Wei, Yong-Hyun Kim,[†] Calvin Curtis, and Daniel Blake

National Renewable Energy Laboratory, Golden, Colorado 80401

Received February 6, 2009; E-mail: hongjun_xiang@nrel.gov

Abstract: It is a challenge to synthesize clusters having a certain shape associated with a desirable property. In this study, we perform density functional calculations on ligand-protected Al₇ and Al₇₇ clusters. It is found that small ligands such as NH₂ still prefer the compact structure of bare Al clusters. However, large ligands such as N(SiMe₃)₂ stabilize the experimentally observed shell-like structures due to the steric effect. This is different from the Ga₈₄ cluster case where small ligands can stabilize the experimental shell-like Ga₈₄ cluster. Our study suggests that the shape, and thus the properties, of clusters (for instance, C_{3v}Al₇ cluster has a finite dipole moment in contrast to the centrosymmetric D_{3d} cluster) can be controlled by using ligands with different sizes.

Introduction

Metal clusters are increasingly the subject of investigation by experimentalist and theoretician because of their special properties in the transitional region between molecular and solid-state chemistry. As aluminum is the most earth abundant metal element with 8.1 wt % and has found many uses in everyday life, nanoclusters of aluminum have been attracting a lot of attention because of their potential mass-production applications in microelectronics¹ and nanocatalysis.^{2,3} Extensive theoretical studies have been performed to search the ground-state structures of small Al_n clusters.^{4–12} Al_n clusters with $n \leq 5$ were found to be planar.⁴ The lowest-energy structures for Al_n with $n = 6–10$ are all based on the octahedron of Al₆ which serves as the nucleation center for the growth of these clusters.^{8,10} When $n \geq 23$, Al_n clusters tend to have a bulklike motif with close-packed (111) facets to obtain lower surface energy and fewer dangling bonds.¹²

Experimentally, crystals containing ligand-passivated Al clusters^{13–15} have been synthesized and characterized by the

X-ray diffraction.¹⁶ The bulky ligands such as N(SiMe₃)₂ (Me = –CH₃) were used to protect the Al clusters from reacting with each other. These ligand-protected Al clusters are called as “metalloid clusters” because there are more metal–metal bonds than metal–ligand bonds. Interestingly, the Al core of these metalloid clusters does not preserve the geometrical feature of the bare Al clusters. In [Al₇{N(SiMe₃)₂}][–], the central Al atom is surrounded by a distorted octahedron of six further Al atoms, each of which is saturated with one N(SiMe₃)₂ ligand.¹³ The arrangement of seven Al atoms is dramatically different from that in the lowest-energy structure of bare Al₇ where an additional Al atom bonds with three Al atoms of the Al₆ octahedron.¹⁰ The [Al₇₇{N(SiMe₃)₂}]₂₀^{2–} cluster has a shell-like structure:¹⁵ it has a central Al atom surrounded by three concentric polyhedral shells containing 12, 44, 20 Al atoms. [Al₆₉{N(SiMe₃)₂}]₁₈^{3–} has a similar onion-like structure.¹⁴ The shell-like structures of Al_n clusters with $n \geq 23$ are unusual because it is expected that the ground-state structures of bare Al₆₉ and Al₇₇ should have a face-centered cubic (fcc) bulk-like motif.¹² Besides the N(SiMe₃)₂ ligand, the Cp* [C₅(CH₃)₅] ligand was used to prepare the metalloid cluster, i.e., Al₅₀ Cp*₁₂.¹⁷ In the center of the metalloid cluster, there is an Al₈ moiety with a distorted square-based antiprism geometry. The different topologies of Al atoms was tentatively attributed to the electronic and steric effects of the ligands.¹⁸ The difference between the Al core of the metalloid clusters and bulk fcc Al was also discussed in terms of the mean atomic volume.^{14,19} However, it remains a mystery why the ligand-protected Al clusters have such unusual and interesting structures.

In this report, we perform density functional calculations on the ligand-protected Al_n clusters to address this issue. Our

[†] Graduate School of Nanoscience and Technology (WCU), Korea Advanced Institute of Science and Technology, Daejeon 305-701, Korea.

- (1) Orlov, A. O.; Amlani, I.; Bernstein, G. H.; Lent, C. S.; Snider, G. L. *Science* **1997**, *277*, 928.
- (2) Valden, M.; Lai, X.; Goodman, D. W. *Science* **1998**, *281*, 1647.
- (3) Roach, P. J.; Woodward, W. H.; Castleman, A. W., Jr.; Reber, A. C.; Khanna, S. N. *Science* **2009**, *323*, 492.
- (4) Jones, R. O. *Phys. Rev. Lett.* **1991**, *67*, 224.
- (5) Yi, J. Y.; Oh, D. J.; Bernholc, J. *Phys. Rev. Lett.* **1991**, *67*, 1594.
- (6) Cheng, H. P.; Berry, R. S.; Whetten, R. L. *Phys. Rev. B* **1991**, *43*, 10647.
- (7) Khanna, S. N.; Jena, P. *Phys. Rev. Lett.* **1992**, *69*, 1664.
- (8) Akola, J.; Hakkinen, H.; Manninen, M. *Phys. Rev. B* **1998**, *58*, 3601.
- (9) Ahlrichs, R.; Elliott, S. D. *Phys. Chem. Chem. Phys.* **1999**, *1*, 13.
- (10) Chuang, F.-C.; Wang, C. Z.; Ho, K. M. *Phys. Rev. B* **2006**, *73*, 125431.
- (11) Li, Z. H.; Jasper, A. W.; Truhlar, D. G. *J. Am. Chem. Soc.* **2007**, *129*, 14899.
- (12) Sun, J.; Lu, W.-C.; Li, Z.-S.; Wang, C. Z.; Ho, K. M. *J. Chem. Phys.* **2008**, *129*, 014707.
- (13) Purath, A.; Köppe, R.; Schnöckel, H. *Angew. Chem., Int. Ed.* **1999**, *38*, 2926.
- (14) Köhnllein, H.; Purath, A.; Klemp, C.; Baum, E.; Krossing, I.; Stösser, G.; Schnöckel, H. *Inorg. Chem.* **2001**, *40*, 4830.

- (15) Ecker, A.; Weckert, E.; Schnöckel, H. *Nature* **1997**, *387*, 379.
- (16) Burgert, R.; Schnöckel, H. *Chem. Commun.* **2008**, 2075.
- (17) Vollet, J.; Hartig, J. R.; Schnöckel, H. *Angew. Chem., Int. Ed.* **2004**, *43*, 3186.
- (18) Schnöckel, H. *Dalton Trans.* **2008**, 4344.
- (19) Schnepf, A.; Schnöckel, H. *Angew. Chem., Ed. Int.* **2002**, *41* (19), 3533.

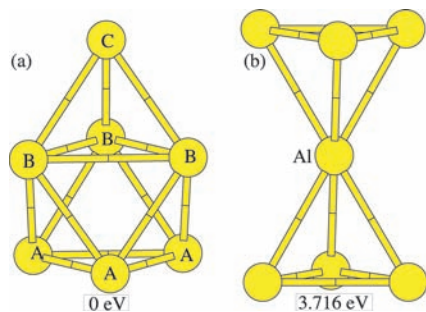


Figure 1. (a) Ground-state Al_7 cluster (point group: C_{3v}) and (b) the Al_7 cluster (point group: D_{3d}) derived from the observed $[\text{Al}_7\{\text{N}(\text{SiMe}_3)_2\}_6]^-$ cluster. The numbers give the relative energies. Here A, B, and C in (a) denote three inequivalent Al sites in the C_{3v} cluster.

theoretical investigations lead to a deeper understanding of the interactions between the ligands and the Al core.

Computational Method

Our first-principles density functional theory (DFT) calculations were performed on the basis of the projector augmented wave method²⁰ encoded in the Vienna ab initio simulation package²¹ using the generalized-gradient approximation (GGA)²² and the plane-wave cutoff energy of 400 eV. For relaxed structures, the atomic forces are less than 0.05 eV/Å. Cubic supercells with large lattice constants ($a = 20$ Å and 30 Å for Al_7 and Al_{77} , respectively) were adopted. The energy correction from the dipole–dipole interaction was found to be less than 1 meV. Except for the isolated NH_2 and $\text{N}(\text{SiMe}_3)_2$, spin-unpolarized calculations were performed. For bare metal clusters, we only consider the neutral charge state. The experimentally determined charge state of the ligand-protected cluster was used in the calculations. However, test calculations on neutral clusters lead to a similar conclusion.

Al_7 Cluster

For simplicity, we first focus on the Al_7 cluster. For the bare Al_7 cluster, the ground-state structure has the C_{3v} symmetry, as shown in Figure 1a. The seven Al atoms of the $[\text{Al}_7\{\text{N}(\text{SiMe}_3)_2\}_6]^-$ cluster displays the D_{3d} symmetry (Figure 1b). Our calculation shows that the C_{3v} cluster is more stable by 3.716 eV than the D_{3d} cluster, confirming the ground-state nature of the C_{3v} cluster. We note that C_{3v} Al_7 cluster has a finite dipole moment (about 0.8 D) in contrast to the centrosymmetric D_{3d} cluster.

Now, we discuss the effect of ligand protection on the relative stability of the Al_7 cluster. As a first step, we consider the NH_2 ligand which has a similar electronic property as $\text{N}(\text{SiMe}_3)_2$. It is noted that the NH_2 ligand was adopted by others to simulate the electronic property of the $\text{N}(\text{SiMe}_3)_2$ protected Al cluster.¹³ For the C_{3v} Al_7 cluster, all Al atoms are exposed to the surfaces and are able to bond with ligands. Due to the symmetry, there are only three inequivalent Al sites (we refer these three inequivalent Al sites as A, B, and C, which are four-, five-, and three-fold coordinated, respectively). Therefore, there are only three possible NH_2 -protected isomers of the $[\text{Al}_7\{\text{NH}_2\}_6]^-$ cluster based on the C_{3v} Al_7 cluster (considering only the on-top configurations, shown in Figure 2a–c). Replacing the $\text{N}(\text{SiMe}_3)_2$ ligand of the experimental structure by NH_2 , we

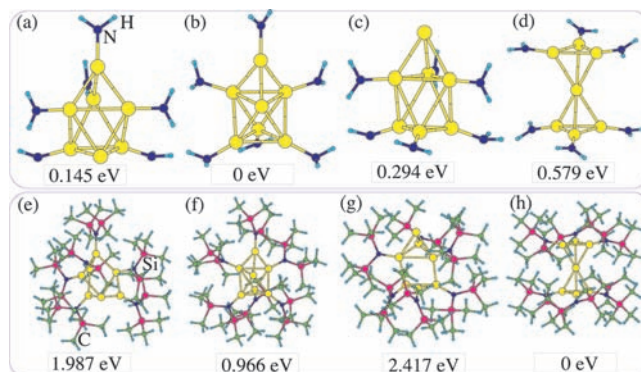


Figure 2. Upper panel shows the isomers of the $[\text{Al}_7\{\text{NH}_2\}_6]^-$ cluster. (a–c) Based on the C_{3v} Al cluster (Figure 1a) with a naked Al atom at A, B, and C sites, respectively. (d) Based on the D_{3d} Al cluster (Figure 1b). Lower panel shows the corresponding isomers of the $[\text{Al}_7\{\text{N}(\text{SiMe}_3)_2\}_6]^-$ cluster.

obtain another isomers of the $[\text{Al}_7\{\text{NH}_2\}_6]^-$ cluster (shown in Figure 2). Our calculation shows that all isomers based on the C_{3v} Al_7 cluster have lower energy than the isomer based on the D_{3d} cluster. The most stable isomer of the $[\text{Al}_7\{\text{NH}_2\}_6]^-$ cluster is the structure with one five-fold coordinated B site Al atom unpassivated. We can also see that after passivated by six NH_2 ligands, the energy difference between the C_{3v} Al cluster and the D_{3d} Al cluster decreases by about 3 eV. To understand the origin of this energy decrease, we calculate the binding energy between a NH_2 ligand and the Al_7 cluster: $E_b = E(\text{NH}_2) + E(\text{Al}_7) - E([\text{Al}_7\text{NH}_2])$. Here we fix the positions of all Al atoms to avoid the large deformation of the Al cluster to obtain a well-defined binding energy on a given Al site. We find that the binding energies for the C_{3v} Al_7 cluster are 3.401, 3.352, and 4.119 eV for the adsorption on the A, B, and C sites, respectively. And for the D_{3d} Al_7 cluster, the binding energy is 4.125 eV. Thus, we can see that the binding energy depends on the coordination number of the Al atom that the ligand is bonded with. For smaller coordinated Al sites, the binding energy is larger. Especially for the three-fold coordinated Al sites (C site in the C_{3v} cluster, and the surrounding Al atoms in the D_{3d} cluster), the binding energy is larger than four- and five-fold coordinated Al sites by about 0.7 eV. This could be attributed to an easier charge transfer from the Al atom with a smaller coordination number to NH_2 . The charge transfer from Al to N atoms was found in the study of $\text{Al}_{77}\text{N}_{20}$.²³ The adsorption energy on the four-fold coordinated Al site (A) is slightly larger than that on the five-fold coordinated Al site (B). This explains why one of the B sites is naked when there are six NH_2 ligands.

Above, we found that the C_{3v} cluster is still more stable than the D_{3d} cluster after NH_2 ligand protection, which is against the experimental observation, although the energy difference is reduced. So, we considered the Al_7 cluster with the real ligand $\text{N}(\text{SiMe}_3)_2$. To our best knowledge, such calculations have never been attempted in previous studies. Similar to our above calculations, we considered three different isomers for the C_{3v} cluster, as shown in Figure 2e–g. Interestingly, the experimental structure with the D_{3d} Al cluster has a lower energy by at least 0.9 eV than the isomers based on the C_{3v} cluster. Also, similar to the NH_2 ligand case, the isomer with a naked B site Al atom is most stable among the isomers based on the C_{3v} cluster. The

(20) (a) Blöchl, P. E. *Phys. Rev. B* **1994**, *50*, 17953. (b) Kresse, G.; Joubert, D. *Phys. Rev. B* **1999**, *59*, 1758.

(21) Kresse, G.; Furthmüller, J. *Comput. Mater. Sci.* **1996**, *6*, 5. Kresse, G.; Furthmüller, J. *Phys. Rev. B* **1996**, *54*, 11169.

(22) Perdew, J. P.; Burke, K.; Ernzerhof, M. *Phys. Rev. Lett.* **1996**, *77*, 3865.

(23) Gong, X. G.; Sun, D. Y.; Wang, X. Q. *Phys. Rev. B* **2000**, *62*, 15413.

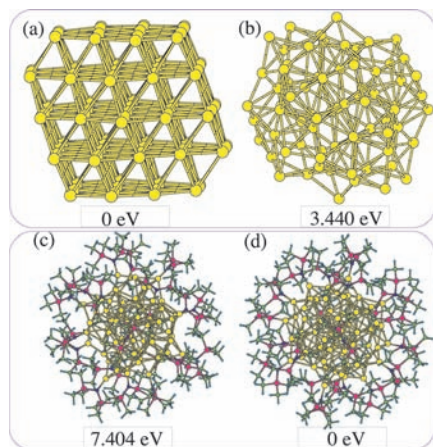


Figure 3. (a) Quasi-fcc-like ground-state structure of Al_{77} and (b) the shell-like structure derived from the observed $[\text{Al}_{77}\{\text{N}(\text{SiMe}_3)_2\}_{20}]^{2-}$ cluster. (c, d) Optimized structures of the $[\text{Al}_{77}\{\text{N}(\text{SiMe}_3)_2\}_{20}]^{2-}$ clusters based on the fcc-like structure and shell-like structure, respectively. The numbers give the relative energies between the isomers.

optimized structures of the C_{3v} -derived Al_7 isomers show that some Al–Al bonds are broken, and thus the Al clusters are largely distorted. This is due to the strong repulsion between neighbor ligands and between Al atoms and closed-shell atoms (not the N atom) of the ligand. We note that the difference between NH_2 and $\text{N}(\text{SiMe}_3)_2$ in stabilizing the Al clusters is not due to their chemical difference because the binding energy of $\text{N}(\text{SiMe}_3)_2$ on the Al clusters is almost the same as that of NH_2 in the absence of space restriction [the binding energy of $\text{N}(\text{SiMe}_3)_2$ on the three coordinated Al sites (both the C site of the C_{3v} cluster and surrounding Al atoms of the D_{3d} cluster) is about 4 eV, which is only 0.1 eV smaller than that of NH_2]. Thus, the stability of the experimental structure is actually due to the steric effect.

Al_{77} Cluster

Next we try to see if similar situation occurs in the ligand protected Al_{77} cluster, which is the largest Al cluster whose structure has been resolved experimentally.¹⁵ The study of this large cluster also helps to provide insights into the crossover between molecular species and the bulk metal. Since the ground state of the bare Al_{77} cluster is not known, we construct a quasi-ground state of the bare Al_{77} cluster by maximizing the Al–Al bonds with the fcc Al framework. This is achieved by the Monte Carlo simulation.²⁴ The resulting structure possesses the (111) fcc facets, as shown in Figure 3a. Our calculation shows that the fcc-based structure has a lower energy than the bare shell-like Al cluster of the experimental structure by 3.440 eV. After passivating some lowest-coordinated Al sites with NH_2 , the energy difference between the $[\text{Al}_{77}\{\text{NH}_2\}_{20}]^{2-}$ clusters decreases to 1.360 eV. To construct a model of the $[\text{Al}_{77}\{\text{N}(\text{SiMe}_3)_2\}_{20}]^{2-}$ cluster based on the fcc-like Al_{77} cluster, we select surface Al atoms that are far from each other to bond with the $\text{N}(\text{SiMe}_3)_2$ ligands. The results show that the experimental structure has a lower energy by 7.404 eV than the fcc-based model cluster. We can see a huge distortion of the fcc-based cluster: The Al core no longer resembles the fcc Al bulk, and the Al atoms bonded with the $\text{N}(\text{SiMe}_3)_2$ ligands move outward from the surface, resembling the shell-like cluster. In

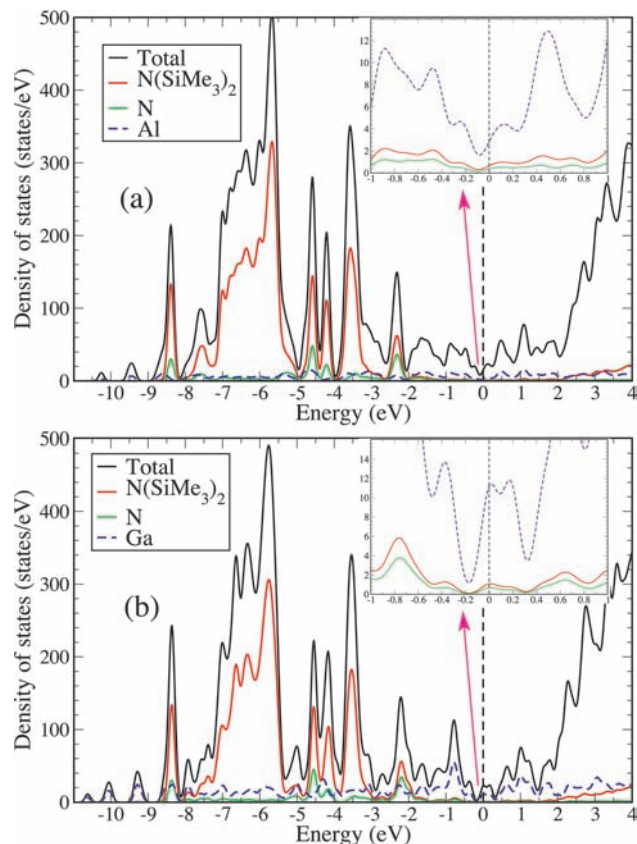


Figure 4. Density of states of the experimental (a) $[\text{Al}_{77}\{\text{N}(\text{SiMe}_3)_2\}_{20}]^{2-}$ cluster and (b) $[\text{Ga}_{84}\{\text{N}(\text{SiMe}_3)_2\}_{20}]^{4-}$ cluster. The partial DOSs for $\text{N}(\text{SiMe}_3)_2$, N, and Al (Ga) are also shown. (Inset) Enlarged plot of the DOS near the Fermi level. The DOS was calculated with 0.1 eV broadening.

contrast, the Al atoms move little when passivated with NH_2 in form of $[\text{Al}_{77}\{\text{NH}_2\}_{20}]^{2-}$. This evidences the steric effect.

The basic electronic structure of the experimental $[\text{Al}_{77}\{\text{N}(\text{SiMe}_3)_2\}_{20}]^{2-}$ cluster is shown in Figure 4a in terms of the density of states (DOS). The valence states from the $\text{N}(\text{SiMe}_3)_2$ ligands locate between -9 to -2 eV. It is found that the large DOS between -8 and -5 eV is contributed from CH_3 groups. The hybridization between Al and N mostly occurs around -4.5 and -2.3 eV. The system is metallic with the states around the Fermi level contributed mostly from Al atoms, and the stability could not be explained in terms of the jellium model²⁰ because the total number of electrons of the cluster is odd. Instead, the DOS displays a pseudo gap around the Fermi level, which is consistent with the stability of the cluster.

The Al valence state in the $[\text{Al}_{77}\{\text{N}(\text{SiMe}_3)_2\}_{20}]^{2-}$ cluster is an interesting issue. Nominally, the average valence state for Al is $(20 - 2)/77 = 0.234$. However, there are many different kinds of Al atoms. As mentioned above, the central Al atom is enclosed by three polyhedral shells containing 12, 44, 20 Al atoms. To characterize the valence state from first-principles, we perform the charge-transfer analysis for the $[\text{Al}_{77}\{\text{N}(\text{SiMe}_3)_2\}_{20}]^{2-}$ cluster through Bader analysis.²⁵ Our result is shown in Figure 5. The center Al atom has a +0.15 valence. Each of the 20 Al atoms of the outer shell loses almost 0.9 electron due to the formation of Al–N bonds. For the first (12-Al atoms) and second Al (44-Al atoms) shells, the valence state

(24) Akola, J.; Manninen, M.; Häkkinen, H.; Landman, U.; Li, X.; Wang, L.-S. *Phys. Rev. B* **2000**, *62*, 13216.

(25) Bader, R. F. W. *Atoms in Molecules: A Quantum Theory*; Oxford University Press: Oxford, 1990.

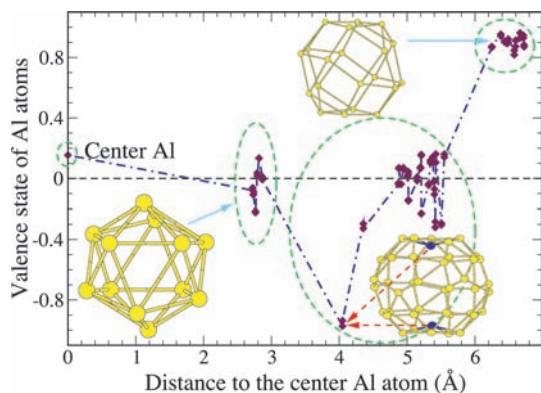


Figure 5. Valence states of Al atoms of the experimental $[\text{Al}_{77}\{\text{N}(\text{SiMe}_3)_2\}_{20}]^{2-}$ cluster from Bader's charge analysis. The central Al atom, and three shells are enclosed by ellipses. The innermost two Al atoms of the 44-Al atoms shell are denoted by blue balls.

can be either negative or positive. The 12-Al atoms shell gains 0.47 electron in total with the magnitude of the valence less than 0.23. Interestingly, two innermost Al atoms of the 44-Al atoms shell gain as many as 0.94 electron. Overall, the second shell gains 3.08 electrons. The complicated valence distribution of the Al atoms is surprising and interesting since one might expect that all Al atoms should have a positive valence between 0 and 1, and the valence decreases when approaching the center Al atom. Our first-principles calculations reveal a very high degree of mixed valency with the valence ranging from -0.94 to 0.96 and is consistent with an enhanced Coulombic interaction picture. It is noted that a small negative valence (the magnitude less than 0.2 e) of Ga was found in the density functional-based tight binding study³² of $[\text{Ga}_{84}\{\text{N}(\text{SiMe}_3)_2\}_{20}]^{4-}$.

To investigate the effect of different ligands on the stability of the Al_{77} cluster, we also study OH and OSiMe₃ passivated Al_{77} clusters. We choose OH because of the strong binding between OH and the Al cluster: the binding energy for the D_{3d} Al_7 cluster is 4.995 eV, which is larger than that (4.125 eV) between NH_2 and the D_{3d} Al_7 cluster. This is due to the larger electronegativity of O than that of N. And the OSiMe₃ ligand is chosen since it is smaller than $\text{N}(\text{SiMe}_3)_2$, and thus the steric effect is weaker. By replacing the NH_2 ligands of the $[\text{Al}_{77}\{\text{NH}_2\}_{20}]^{2-}$ clusters with OH ligands, we find that the fcc-based $[\text{Al}_{77}\{\text{OH}\}_{20}]^{2-}$ cluster is more stable than the shell-like cluster by 1.753 eV, similar to the NH_2 case. Using the same method of the construction of the fcc-based $[\text{Al}_{77}\{\text{N}(\text{SiMe}_3)_2\}_{20}]^{2-}$ cluster, we obtain a fcc-like $[\text{Al}_{77}\{\text{OSiMe}_3\}_{20}]^{2-}$ cluster. The relaxed structures of $[\text{Al}_{77}\{\text{OSiMe}_3\}_{20}]^{2-}$ clusters are shown in Figure 6. Our calculation shows that the fcc-based $[\text{Al}_{77}\{\text{OSiMe}_3\}_{20}]^{2-}$ cluster has a higher energy than the shell-like structure by 1.720 eV. In this case, the fcc-based cluster is less stable than the shell-like cluster, as in the $\text{N}(\text{SiMe}_3)_2$ case. However, the energy difference is much smaller. This is understandable because of the reduced steric repulsion in the OSiMe₃ case, which can be seen from the fact that the fcc Al core is kept in the relaxed structure of fcc-based $[\text{Al}_{77}\{\text{OSiMe}_3\}_{20}]^{2-}$ cluster (Figure 6a).

Our above calculations considered the ligands which bind strongly to the Al clusters. To understand the interaction between inert ligands and the Al clusters, we carry out some calculations with Al_{77} cluster covered by 20 closed-shell H_2O or $\text{O}(\text{SiMe}_3)_2$ ligands, respectively. In both cases, after structural optimizations, some of the 20 ligands are not bound to the Al cluster, and the fcc-based cluster is always more stable than the shell-like cluster.

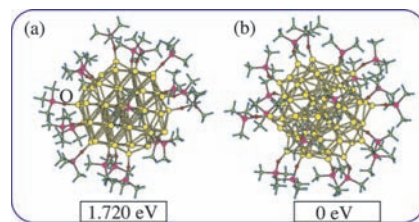


Figure 6. (a and b) Optimized structures of the $[\text{Al}_{77}\{\text{OSiMe}_3\}_{20}]^{2-}$ clusters based on the fcc-like structure and shell-like structure, respectively. The numbers give the relative energies between the isomers.

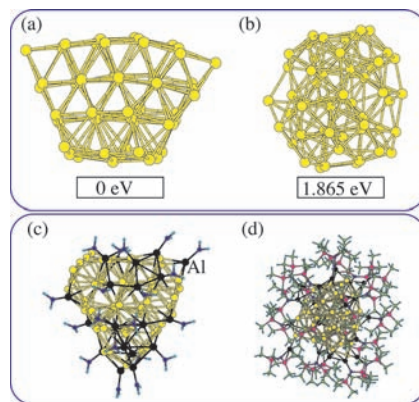


Figure 7. (a) Quasi-fcc-like ground-state structure of bare Al_{57} and (b) the shell-like Al_{57} structure derived from the observed $[\text{Al}_{77}\{\text{N}(\text{SiMe}_3)_2\}_{20}]^{2-}$ cluster. (c, d) Optimized structures of the $[\text{Al}_{77}\{\text{NH}_2\}_{20}]^{2-}$ and $[\text{Al}_{77}\{\text{N}(\text{SiMe}_3)_2\}_{20}]^{2-}$ clusters obtained by passivating the fcc-like bare Al_{57} cluster using 20 Al-NH₂ and Al-N(SiMe₃)₂, respectively. The numbers give the relative energies between the isomers.

Thus, to favor an open structure of the Al cluster, the ligand should be not only bulky but also reactive.

Al_{57} Cluster

By collisions with argon atoms in the gas phase,²⁶ the $[\text{Ga}_{13}(\text{GaR})_6]^-$ cluster²⁷ ($\text{R} = \text{C}(\text{SiMe}_3)_3$) fragments by detaching step by step neutral GaR units and finally leading to the stable 40-electron bare metal cluster $[\text{Ga}_{13}]^-$. This might suggest that Al_{57} could be taken as an alternative bare metal cluster underlying the $[\text{Al}_{77}\{\text{N}(\text{SiMe}_3)_2\}_{20}]^{2-}$, i.e., $[\text{Al}_{57}\{\text{AlN}(\text{SiMe}_3)_2\}_{20}]^{2-}$ cluster. Therefore, we also consider the bare Al_{57} cluster and the passivation of 20 Al-R [$\text{R} = \text{NH}_2$, OH, $\text{N}(\text{SiMe}_3)_2$, OSiMe₃, H_2O , and $\text{O}(\text{SiMe}_3)_2$] groups to the Al_{57} cluster. Extensive first-principles molecular dynamics simulations show that the structure shown in Figure 7a is the ground-state structure of the bare Al_{57} cluster. This fcc-like Al_{57} cluster with distorted fcc (111) facets is more stable by 1.865 eV than the bare Al_{57} cluster [Figure 7b] derived from the experimental $[\text{Al}_{77}\{\text{N}(\text{SiMe}_3)_2\}_{20}]^{2-}$ cluster. After addition of 20 Al-NH₂ to suitable positions of the fcc-like Al_{57} cluster that maximize the number of Al-Al bonds and minimize the strain [Figure 7c], we find the $[\text{Al}_{77}\{\text{NH}_2\}_{20}]^{2-}$ cluster based on the fcc-like Al_{57} cluster has a lower energy by 0.778 eV than that based on the experimental shell-like structure. However, when large ligands, i.e., Al-N(SiMe₃)₂, are bonded to the Al_{57} cluster, the experimental shell-like structure becomes more stable by 8.056 eV than the $[\text{Al}_{77}\{\text{N}(\text{SiMe}_3)_2\}_{20}]^{2-}$ cluster [Figure 7d] based on the

(26) Weiss, K.; Schnöckel, H. *Z. Anorg. Allg. Chem.* **2003**, *629*, 1175.

(27) Schnepf, A.; Stösser, G.; Schnöckel, H. *J. Am. Chem. Soc.* **2000**, *122*, 9178.

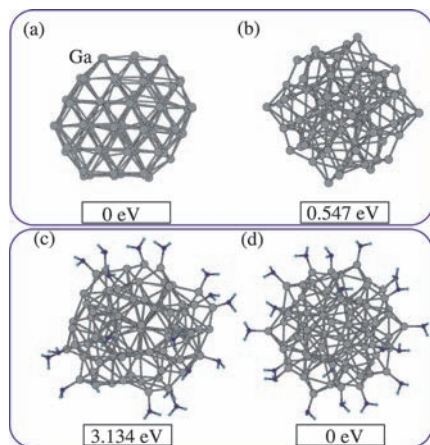


Figure 8. (a) Quasi-fcc-like ground-state structure of Ga_{84} and (b) the shell-like structure derived from the observed $[\text{Ga}_{84}\{\text{N}(\text{SiMe}_3)_2\}_{20}]^{4-}$ cluster. (c, d) Optimized structures of the $[\text{Ga}_{84}\{\text{NH}_2\}_{20}]^{4-}$ clusters based on the fcc-like structure and shell-like structure, respectively. The numbers give the relative energies between the isomers.

fcc-like Al_{57} cluster. The Al-OH and Al-OSiMe_3 cases are similar to Al-NH_2 and $\text{Al-N}(\text{SiMe}_3)_2$ cases, respectively. And for ligands R [$\text{R} = \text{H}_2\text{O}$ and $\text{O}(\text{SiMe}_3)_2$] that are weakly binding to Al , the addition of 20 Al-R to the bare Al_{57} cluster results in a partially dissociated structure. Therefore, using Al_{57} as the starting point leads to qualitatively the same results as we found in the Al_{77} case.

Ga₈₄ Cluster

Recently, Ga (a member of the same group in the periodic table as Al) metalloid clusters have been synthesized besides Al metalloid clusters. Of particular interest is the $[\text{Ga}_{84}\{\text{N}(\text{SiMe}_3)_2\}_{20}]^{4-}$,²⁸ which shows bulk superconductivity below $T_c \approx 8 \text{ K}$ in the crystalline ordered structure.²⁹ It is interesting to compare the $[\text{Ga}_{84}\{\text{N}(\text{SiMe}_3)_2\}_{20}]^{4-}$ cluster to $[\text{Al}_{77}\{\text{N}(\text{SiMe}_3)_2\}_{20}]^{2-}$ because these two clusters have the same number and kind of ligands.

First, we try to find the ground-state structure of the bare Ga_{84} cluster. It is well-known that the element gallium is on the borderline between real metals to semimetals or nonmetals having a great variety of seven different modifications including the fcc Ga . It was found that $\alpha\text{-Ga}$ which can be described as a molecular metal made up of Ga_2 dumbbells has the lowest energy.³⁰ We construct two models of Ga_{84} by maximizing the number of Ga-Ga bonds with the fcc or $\alpha\text{-Ga}$ frameworks. It is found that the fcc-based bare Ga_{84} cluster has a lower energy by about 1.0 eV even though bulk fcc- Ga is less stable than $\alpha\text{-Ga}$. We also choose about 30 geometries from a first-principles molecular dynamics simulation at 1200 K, which are subsequently relaxed until the atomic forces are less than 0.05 eV/Å. However, no local minimum with lower energies than the fcc-based bare Ga_{84} cluster is found. The lowest-energy structure of the bare Ga_{84} cluster from our calculation is shown in Figure 8a. Our calculations show that the fcc-based bare Ga_{84} cluster is more stable than the core Ga_{84} cluster of the experimental $[\text{Ga}_{84}\{\text{N}(\text{SiMe}_3)_2\}_{20}]^{4-}$ cluster by about 0.55 eV. The small energy difference is consistent with the fact that the fcc structure is not the ground state of bulk Ga . We also calculate

the energies of the $[\text{Ga}_{84}\{\text{NH}_2\}_{20}]^{4-}$ clusters made from the fcc-like and experimental Ga_{84} clusters (Figure 8c and d). The results show that the $[\text{Ga}_{84}\{\text{NH}_2\}_{20}]^{4-}$ cluster with the experimental Ga core has a lower energy by 3.13 eV. And the $[\text{Ga}_{84}\{\text{NH}_2\}_{20}]^{4-}$ cluster based on the fcc-like Ga_{84} cluster distorts drastically from the fcc framework. The $\text{N}(\text{SiMe}_3)_2$ ligands covered fcc Ga_{84} cluster is found to be unstable with a very high energy. Thus, the large $\text{N}(\text{SiMe}_3)_2$ ligands further stabilize the more open experimental $[\text{Ga}_{84}\{\text{N}(\text{SiMe}_3)_2\}_{20}]^{4-}$ cluster, in agreement with the experimental observation.²⁹ Comparing the Ga_{84} cluster with the Al_{77} case, we find that the main difference is that small ligands such as NH_2 can stabilize the experimental core Ga cluster but not for the Al_{77} case. This is understandable because of the small energy difference between the bare Ga_{84} clusters. The consideration of the Ga_{64} cluster gives similar results. Thus, the experimental observed Ga_{84} structure should not be attributed to the size effect of the ligands.

For comparison with the $[\text{Al}_{77}\{\text{N}(\text{SiMe}_3)_2\}_{20}]^{2-}$ cluster, we show the electronic DOS of the experimental shell-like $[\text{Ga}_{84}\{\text{N}(\text{SiMe}_3)_2\}_{20}]^{4-}$ cluster in Figure 4b. Similar to the $[\text{Al}_{77}\{\text{N}(\text{SiMe}_3)_2\}_{20}]^{2-}$ cluster case, the DOS of the valence states between -9 and -2 eV is dominated by the contribution from the $\text{N}(\text{SiMe}_3)_2$ ligands. And the DOS near the Fermi level is mostly contributed by Ga atoms. However, there is an important and interesting difference in the DOS around the Fermi level between these two clusters: The Fermi level of the $[\text{Ga}_{84}\{\text{N}(\text{SiMe}_3)_2\}_{20}]^{4-}$ cluster locates at a peak of the DOS, and the $[\text{Ga}_{84}\{\text{N}(\text{SiMe}_3)_2\}_{20}]^{4-}$ cluster has a much larger DOS at the Fermi level than the $[\text{Al}_{77}\{\text{N}(\text{SiMe}_3)_2\}_{20}]^{2-}$ cluster, which might be responsible for the superconductivity observed in the crystalline ordered compound containing $[\text{Ga}_{84}\{\text{N}(\text{SiMe}_3)_2\}_{20}]^{4-}$ clusters.³⁰ We note that there are substantial differences in the DOS of the $[\text{Ga}_{84}\{\text{N}(\text{SiMe}_3)_2\}_{20}]^{4-}$ cluster, especially near the Fermi level, between our result and that computed by the density functional-based tight binding method.³¹

Conclusion

In conclusion, our calculations explain why experiments observed a more open structure of the Al clusters instead of the compact ground-state structure in the presence of large ligands such as $\text{N}(\text{SiMe}_3)_2$. Our study demonstrates that the size of the ligand plays a decisive role in selecting the shape of a cluster. The general results obtained here pave a way of controllable synthesis of clusters with desirable properties (e.g., high catalytic activity)³² by using ligands with different sizes. In addition, our first-principles calculations indicate that some Al atoms of the Al metalloid clusters have unexpectedly large negative valences.

Acknowledgment. This work was supported by the DOE/NREL/LDRD program, under Contract No. DE-AC36-08GO28308. We thank Dr. Xiaojun Wu for useful discussions. Y.H.K. was partly supported by Korea Science and Engineering Foundation (KOSEF) grant funded by the Korean government (MEST) (grant code: R31-2008-000-10071-0).

Supporting Information Available: Absolute energies and optimized geometries of all calculated structures. This material is available free of charge via the Internet at <http://pubs.acs.org>.

JA900965W

(28) Schnepf, A.; Schnöckel, H. *Angew. Chem., Int. Ed.* **2001**, *40*, 711.

(29) Bakharev, O. N.; Bono, D.; Brom, H. B.; Schnepf, A.; Schnöckel, H.; de Jongh, L. J. *Phys. Rev. Lett.* **2006**, *96*, 117002.

(30) Gong, X. G.; Chiarotti, G. L.; Parrinello, M.; Tosatti, E. *Phys. Rev. B* **1991**, *43*, 14277.

(31) Frenzel, J.; Gemming, S.; Seifert, G. *Phys. Rev. B* **2004**, *70*, 235404.

(32) Herzog, A. A.; Kiely, C. J.; Carley, A. F.; Landon, P.; Hutchings, G. J. *Science* **2008**, *321*, 1331.